

Magnetic Resonance Imaging Artifacts

4

Dinesh R. Singh, Helmut Rumpel,
Michael S.M. Chin, and Wilfred C.G. Peh

Contents

4.1	Introduction	61
4.2	MRI Artifacts	62
4.2.1	Motion	62
4.2.2	Susceptibility and Artifacts Related to Orthopedic Hardware	66
4.2.3	Chemical Shift	71
4.2.4	Magic Angle Phenomenon	72
4.2.5	Protocol Errors	73
4.3	Technical Pros and Cons	77
4.3.1	Fat-Suppression Techniques	77
4.3.2	Isotropic Imaging	77
	Conclusion	79
	References	80

Abbreviations

CSF	Cerebrospinal fluid
CT	Computed tomography
EPI	Echo planar imaging
FOV	Field of view
FSE	Fast spin-echo
MRI	Magnetic resonance imaging
RF	Radiofrequency
SNR	Signal-to-noise ratio

D.R. Singh, MBBS, DNB, MMed, FRCR (✉)
M.S.M. Chin, DCR • W.C.G. Peh, MD, FRCPE,
FRCPG, FRCR
Department of Diagnostic Radiology,
Khoo Teck Puat Hospital,
90 Yishun Central, Singapore 768828,
Republic of Singapore
e-mail: Rambachan.singh.dinesh@alexandrahealth.com.sg;
bluevodka99@yahoo.com;
Wilfred.peh@alexandrahealth.com.sg

H. Rumpel, PhD
Department of Diagnostic Radiology,
Singapore General Hospital, Outram Road,
Singapore 169608, Republic of Singapore
e-mail: Helmut.rumpel@sgh.com.sg

4.1 Introduction

Musculoskeletal imaging deals with pathologies of the bones, joints, and surrounding soft tissue structures. A number of imaging modalities are useful in evaluating musculoskeletal pathologies, including radiographs, ultrasound imaging, computed tomography (CT), and magnetic resonance imaging (MRI). All these modalities have a unique role in diagnosing various lesions, ranging from simple fractures to complex neoplasms. MRI is of special importance, as it involves non-ionizing radiation and has excellent soft tissue resolution. Although radiographs and CT are useful in diagnosing fractures and bone destruction, MRI is far superior for detecting lesions involving the bone marrow and in assessing adjacent soft tissue involvement. Newer high-field-strength machines have improved the image quality and have broadened the scope of imaging. Imaging is no longer limited to evaluating the

anatomical details, and functional assessment is possible for many structures. Continuous enhancements in scanning techniques have taken MRI to a new level, making it possible to identify subtle pathologies with shorter scanning times.

MRI is, however, inherently prone to a number of artifacts; some arise from motion, while others are related to technical or external factors (Jiachen and Rao 2006). A number of these artifacts are more pronounced on high-field-strength magnets and can result in suboptimal image quality (Bernstein et al. 2006; Dietrich et al. 2008). Susceptibility artifacts have gained importance with increasing role of MRI in post-operative patients, especially after joint replacement procedures or surgical implants. Some of the artifacts can be limited by simple corrective measures, while others can be significantly reduced using various modifications to the scanning technique. Awareness of these artifacts is essential to avoid possible interpretation pitfalls. There are several other challenges to MRI on new high-field-strength machines. The advent of 3-tesla machines has greatly improved the image resolution and has reduced the scanning times. However, a number of challenges have to be overcome to allow optimal utilization of these machines. Some of these challenges include fat suppression and chemical shift artifacts (Shapiro et al. 2012).

4.2 MRI Artifacts

MRI artifacts can be broadly classified into a few subgroups. Some of the artifacts can be related to motion, which may be due to movement of the patient or even due to periodic motion. Pulsation of the cerebrospinal fluid (CSF), beating of the heart, respiration, and pulsation of the blood vessels are some causes of periodic motion artifacts. Other artifacts can be due to physical or technical factors or may be related to the machine or the scanning technique. External factors like radiofrequency (RF) interference can also cause very characteristic artifacts and can be easily reduced in most cases.

4.2.1 Motion

Motion artifacts are routinely encountered on musculoskeletal imaging. These artifacts are usually related to movement of the patient during the scan and can cause significant degradation of the quality of the MR image (Fig. 4.1). Motion artifacts can be easily recognized, and reduction measures can be applied, depending on the cause. MRI requires an absolutely stationary patient, in order to obtain the best image quality. This may, however, be difficult to achieve, as it is virtually impossible for even the most cooperative of patients to lie absolutely still for the duration of

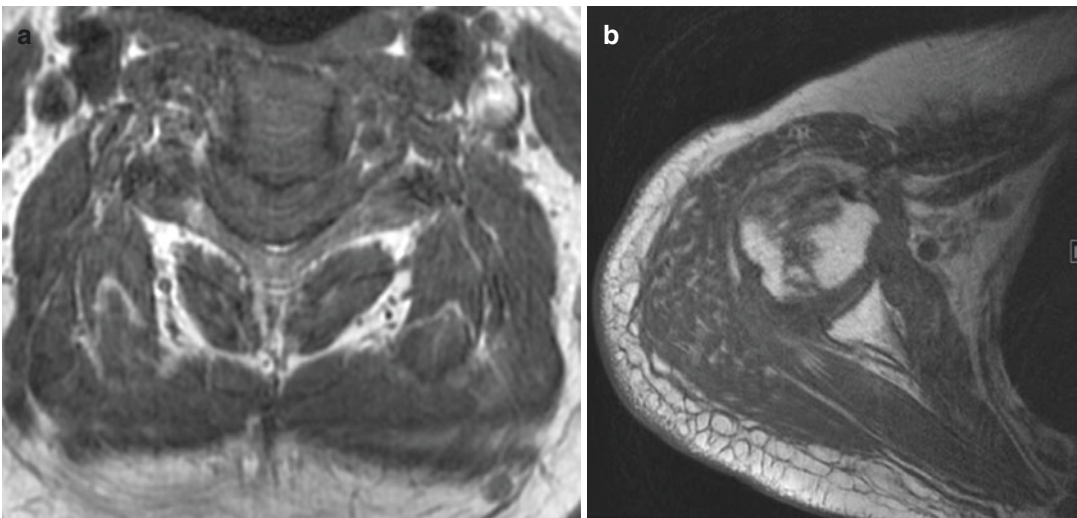


Fig. 4.1 Motion artifact. Axial T1-W MR images of the (a) cervical spine and (b) shoulder show motion artifacts resulting in poor image quality

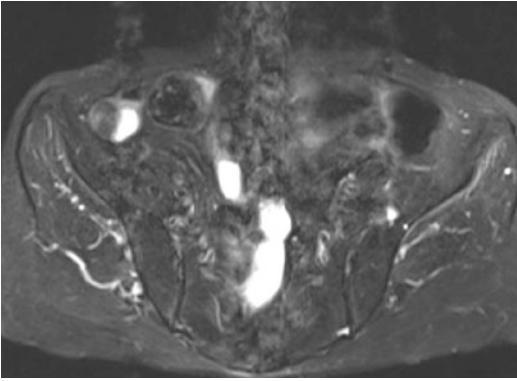


Fig. 4.2 Motion artifact arising from the bowel

the MR scan. Besides the motion related to the patient, there are many other sources of motion artifacts (Smith and Nayak 2010). These may arise from regular motion of structures, such as movement of the lungs during respiration, contraction of the heart, peristalsis of the bowel (Fig. 4.2), or even pulsation of the blood vessels. While it may be possible to restrict patient motion, it is impossible to prevent these above-mentioned causes of motion artifacts. Specific correction methods have to be applied to restrict the effect of these artifacts during the scan.

Motion artifacts are resultant of the phase-encoding gradient being unable to predictably encode the radio waves arising from the moving body structures (Peh and Chan 2001). Motion artifacts depend on factors such as speed of the moving structure and the manner in which the structure is moving. These artifacts become more prominent with increasing magnetic field strengths and are more severe on the newer MRI machines. The corrective measures depend on the cause of the motion artifact, as these can be related to voluntary or involuntary motion. Smearing and ghosting are the most typical artifacts arising from patient motion (Morelli et al. 2011). Artifacts arising from patient motion can be reduced by simple measures like restricting or limiting movement of the patient and with proper counseling before the scan. In pediatric patients, soft pads can be placed between the patient and the inner margin of the coil. Use of Velcro straps can also help in restricting the motion of the imaged body part in an uncooperative patient. In cases where the scan duration is long, simple

measures like reassuring the patient and giving the patient adequate breaks can go a long way in limiting random motion artifacts. Sedation techniques are routinely used in scanning of pediatric cases and can also be used in adult patients.

The use of PROPELLER (periodically rotated overlapping parallel lines with enhanced reconstruction) and Turboprop-MRI can help reduce these motion artifacts as well. The motion correction technique is better because retrospective motion correction can be used in addition (Tamhane and Arfanakis 2009). PROPELLER MRI technique may sometimes result in under-sampling artifacts with uneven blurring in the reconstructed image. This can be overcome by over-sampling and iterative reconstruction (Tamhane et al. 2012).

Periodic motion artifacts can result from cardiac contraction, respiratory motion, vascular pulsation, or peristalsis of the bowel. These artifacts from repetitive motion give rise to ghost images along the phase-encoding direction. The degree of brightness of these ghost images depend on factors like the speed and the amplitude of the periodic motion causing these artifacts. Many techniques have been devised to limit the effect of these artifacts, such as the use of cardiac or respiratory gating, navigator pulse, and faster MR sequences. The use of saturation bands reduces the artifacts from respiratory motion, vascular and esophageal peristalsis (Fig. 4.3). In sagittal cervical spine MRI, a saturation pulse can be applied parallel to the spine anteriorly, and this can reduce these artifacts.

CSF can cause pulsation artifacts and is typically encountered in MRI of the spine. These artifacts are more prominent as the CSF space gets bigger and are often visualized in MRI of the thoracic spine. These artifacts can easily be misinterpreted as lesions involving the spinal canal. CSF pulsation artifacts result in formation of ghost images, seen along the phase-encoding direction, and are visualized as hypointense signal areas on T2-weighted images (Singh et al. 2014). These T2-hypointense signal foci can easily mimic a flow void arising from a vascular malformation. The use of gradient-echo sequences results in reduction of these artifacts and can be used as a problem-solving tool in difficult cases (Fig. 4.4).

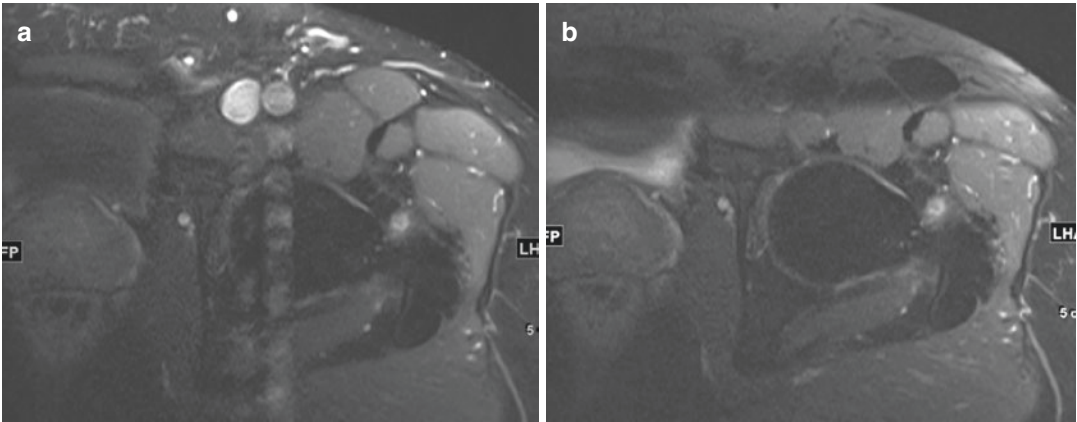


Fig. 4.3 Arterial pulsation artifact. Axial contrast-enhanced fat-suppressed T1-W MR images of the hip show (a) pulsation artifact from the left femoral artery, which is (b) reduced by using a saturation band over the vessel

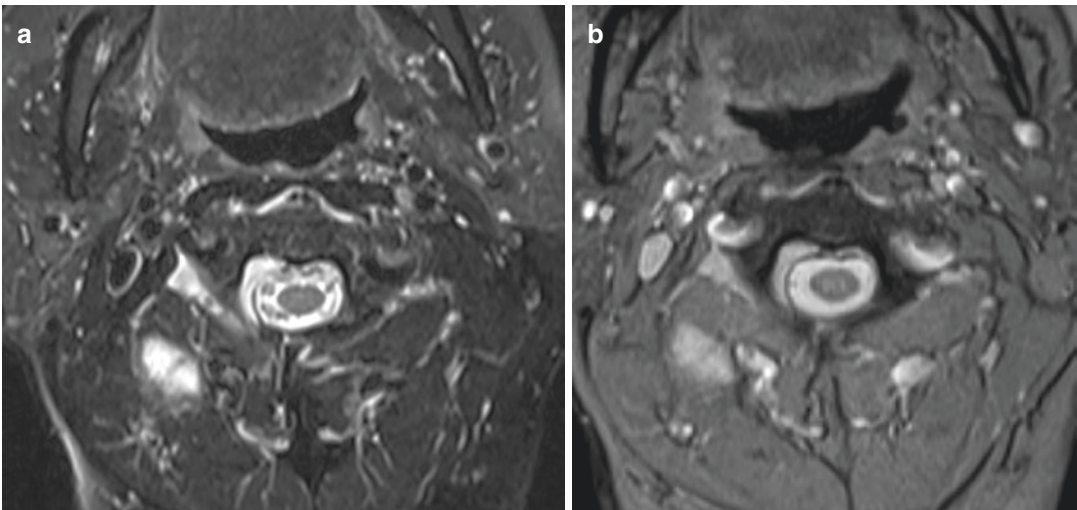


Fig. 4.4 CSF pulsation artifact. (a) Axial fat-suppressed T2-W MR image of the cervical spine shows CSF pulsation artifact. (b) The artifact is reduced on the gradient-echo image

CSF pulsation artifacts have also been found to be useful, and there is limited evidence to show that absence of these artifacts can be used as an indicator of cord compression.

Motion artifacts can also arise from flowing blood in the vascular structures and result in signal flow voids, typically seen on T2-weighted sequences. These artifacts can be useful in diagnosing vascular malformations of the spine or the soft tissue structures. The absence of these flow voids is a good indicator of an underlying vascular thrombosis. Motion artifacts arising from the blood vessels can be seen as ghost images in pulsatile flow or as high-signal areas on gradient-

echo sequences in continuous blood inflow (Peh and Chan 2001). These artifacts can be reduced by using flow compensation techniques and saturation bands or by switching the phase- and frequency-encoding directions (Singh et al. 2014). The application of additional gradient pulses minimizes the phase shifts from moving protons and rephases the signal from stationary protons. This is termed as gradient moment nulling (Morelli et al. 2011). This technique can be combined with the penalty of longer echo time (TE). The use of saturation pulse is another technique that can be used in reducing pulsation artifact. This technique uses an additional RF pulse,

applied either parallel or perpendicular to the imaging plane. The most common use is in imaging of the spine, where a saturation pulse is applied anterior and parallel to the spine, to reduce pulsation-related motion artifacts. Similar to this, a saturation pulse can also be applied over a blood vessel, to reduce its pulsation artifact.

With advancement in technology, a number of newer MR scanning sequences have been devised, which have much shorter scan times without significant compromise in the image quality. MR scan time has also been significantly shortened with other advancements, such as the use of different image acquisition techniques, improvement in the coil technology (multichannel coils), higher-field-strength magnets, and improvement in the gradient strength (Morelli et al. 2011). Some of these newer image acquisition techniques include single-shot single-section imaging, multi-section imaging and parallel imaging (Singh et al. 2014). Spin-echo imaging technique is relatively insensitive to inhomogeneity in the magnetic field and has been most widely used. Fast spin-echo (FSE) techniques result in significant reduction in acquisition times; however, excessive echo train length may result in many artifacts and blurring of the image. Multi-section imaging also reduces the image acquisition time by simultaneous imaging of several interleaved sections (Morelli et al. 2011). This technique is however more susceptible to patient motion artifacts. This drawback is overcome by the use of single-shot single-section imaging techniques, which are more robust in relation to patient-motion artifacts. Techniques like HASTE (half-Fourier single-shot turbo spin echo) are excellent in reducing motion artifacts, as acquisition times are close to freezing motion. These are however more susceptible to other types of artifacts. The PROPELLER technique allows reduction of various motion artifacts encountered on MRI of the musculoskeletal system (Dietrich et al. 2011).

Fast gradient-echo sequences and steady-state sequences use shorter repetition time (TR) and result in reduced scan time. These sequences result in excellent signal-to-noise ratio (SNR) and better contrast in comparison to spoiled gradient-echo sequences (Chavhan et al. 2008).

Post-excitation refocused steady-state sequences are especially useful in evaluating menisci and the cartilage. Pre-excitation refocused steady-state sequences are useful in evaluation of the spine (Chavhan et al. 2008). Modified fully refocused steady-state sequences are useful in evaluation of the brachial plexus and the spine. The DESS (double-echo steady-state) sequence is useful in evaluation of the articular cartilage. Echo planar imaging (EPI) is a fast imaging technique that is capable of freezing motion to a large extent. It allows extremely fast image acquisition by acquiring all the spatial encoding information with a single RF excitation. Single-shot EPI acquires the entire range of phase-encoding steps in one TR. Segmented EPI in phase reduces the train length, while readout-segmented EPI reduces the inter-echo time. Any difference in susceptibility, as from local tissue to bone, leads to a magnetic field gradient and will result in substantial image distortions. Readout-segmented EPI is useful in evaluation of the vertebra and the spinal cord and can be helpful in differentiating benign from metastatic compression fractures (Rumpel et al. 2013).

Parallel imaging is a method for encoding the MR signal that allows reduction in the scan time, due to a reduced number of phase-encoding steps needed to form the image. This technique is especially useful in musculoskeletal MRI (Shapiro et al. 2012) and uses multichannel multicoil technology, where signal from different regions is received by different coils with known efficiency. Parallel imaging reduces the scanning time by reducing the number of phase-encoding steps, depending on a parallel imaging factor. Parallel imaging uses special image reconstruction algorithms, such as sensitivity encoding (SENSE), generalized autocalibrating partially parallel acquisition (GRAPPA), partially parallel imaging with localized sensitivity, and integrated parallel acquisition techniques (Singh et al. 2014). Although parallel imaging is useful in reducing scan time, there is reduction in the overall SNR with compromise in the image uniformity. Artifacts can be seen on parallel imaging, such as noise enhancement and residual aliasing (Deshmane et al. 2012). Noise enhancement makes the structures appear grainy, the severity

of which varies across the image. Residual aliasing may arise due to inaccurate coil sensitivity map and can be seen if the patient moves after the initial planning scan. It can also be seen with errors in the GRAPPA weights. This can result in a bright ridge in the region of interest, especially seen when the edge of the object is bright (Deshmane et al. 2012). These artifacts can be reduced by optimization of the parallel imaging parameters and by choosing the appropriate reconstruction algorithm and the coil array.

4.2.2 Susceptibility and Artifacts Related to Orthopedic Hardware

MRI is susceptible to artifacts arising due to inhomogeneity of the magnetic field. This may be due to inhomogeneous distribution of the main magnetic field or may be due to external factors related to the patient, causing the field inhomogeneity. Magnetic susceptibility is described as the degree of magnetization of a structure or an object, when placed in an external magnetic field. When this occurs, a structure produces a magnetic field on its own, the degree and nature of which depend on its inherent properties. The magnetic field contribution may be in or opposite to the direction of the main magnetic field, depending on whether the structure is paramagnetic or diamagnetic. The degree of magnetic susceptibility is directly proportional to the strength of the external magnetic field (Dietrich et al. 2008). As a result, the magnetic susceptibility artifacts are stronger on higher-field-strength magnets. Different structures have different magnetic susceptibilities, and susceptibility artifacts typically arise at the interface of the structures, due to magnetic field inhomogeneity. This causes magnetic field distortion and results in spatial misregistration (Peh and Chan 2001).

There are various causes for susceptibility artifacts on MRI. The presence of dental prostheses can severely affect the image quality in imaging of the head and neck (Eggers et al. 2005). Susceptibility artifacts are commonly seen when imaging a joint with underlying metallic prosthesis (Hargreaves et al. 2011). They are also seen around metallic clips or fine metallic debris.

Susceptibility artifacts are known to be stronger with some metals. Titanium alloy implants are known to cause less severe susceptibility artifacts, compared to stainless steel implants (Lee et al. 2007). The severity of the magnetic susceptibility artifacts also depends on the type of sequences used for scanning. Gradient-echo sequences result in more severe metal susceptibility artifacts and in an exaggerated hypointense signal around the metallic object. This phenomenon is known as blooming and often results in a distorted image, with the soft tissues appearing smaller and the bone appearing disproportionately larger. These blooming artifacts can very easily be misinterpreted as an abnormality, thereby resulting in a misdiagnosis. Hypointense signal from the susceptibility artifacts arising from small metallic objects or debris in the spine can be misinterpreted as abnormal bone or thecal sac signal. In joint imaging, similar small foci can be misinterpreted as pseudolesions, especially the susceptibility artifacts caused by air bubbles on MR arthrography.

Susceptibility artifacts have become more important with the increasing use of MRI in the postoperative spine and in patients with metallic implants (Cha et al. 2011; Mansson et al. 2015) (Fig. 4.5). CT has a limited role in these cases, with limited assessment of the soft tissue structures and the bone marrow. The presence of metallic objects also causes beam hardening artifacts on CT, thereby causing further problems in accurate assessment (Lee et al. 2007). The severity of these artifacts depends on the field strength, and hence, these artifacts are more prominent on 3 T compared to 1 T or 1.5 T machines (Bernstein et al. 2006). There has been a progressive increase in the number of joint replacement procedures, mainly involving the hip and the knee joints. The use of metallic orthopedic hardware can result in artifacts on MRI that can be seen both in the primary imaging plane (in-plane artifacts) and in the adjacent planes (through-plane artifacts). The main artifact types are signal pileup or loss, insufficient inversion, and displacement artifacts (Sutter et al. 2012). The use of fat-suppression techniques in these cases can result in failure of fat and water suppression around, and even away, from the metallic hardware. Specific correction measures have to be

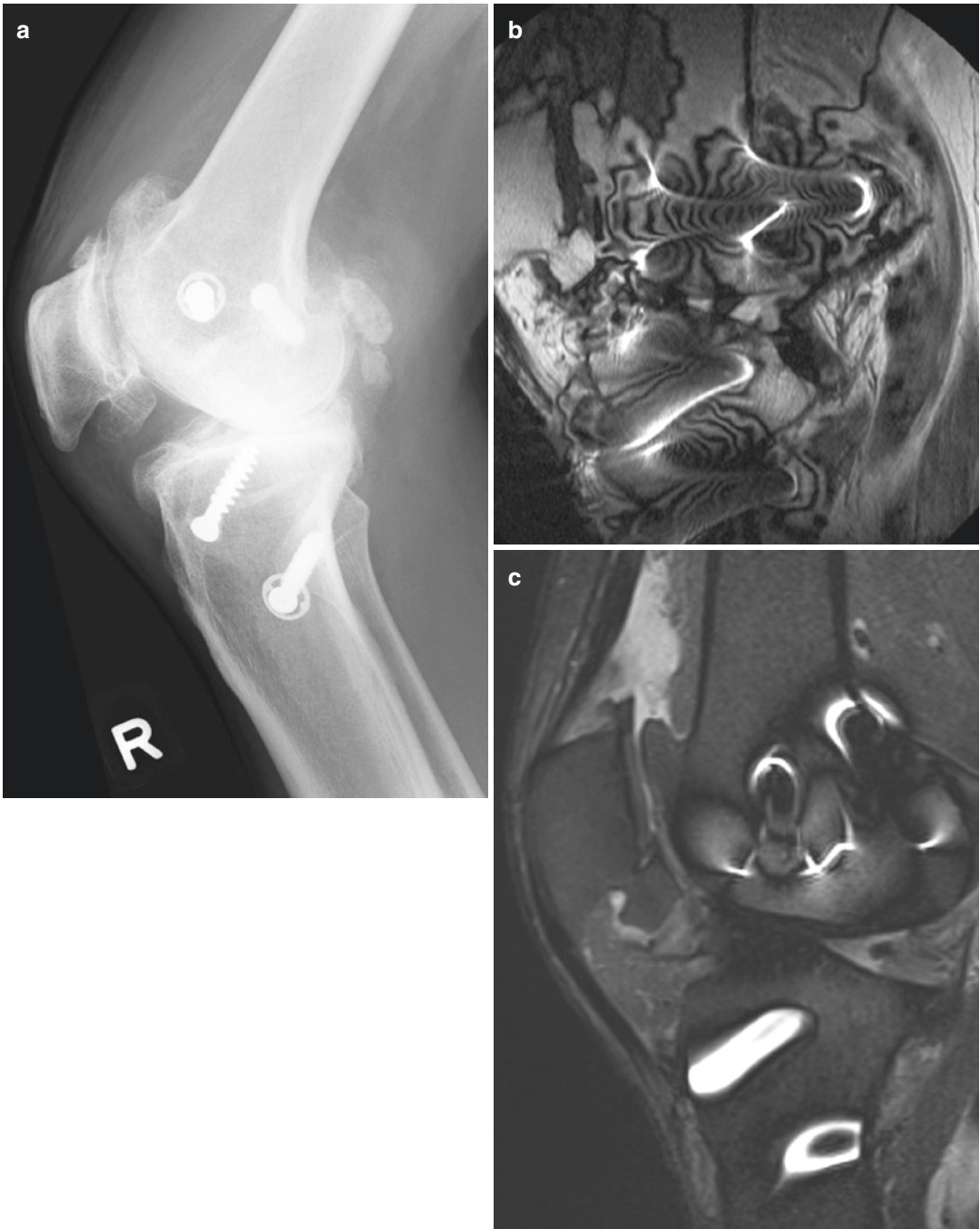


Fig. 4.5 Susceptibility artifacts. (a) Lateral radiograph of the knee shows reconstruction screws located in the distal femur and tibia. (b) Sagittal fat-suppressed PD-W MR

image shows severely compromised image quality due to these screws. (c) There is marked improvement in the image quality on TIRM sagittal image

applied to reduce these artifacts and are discussed in the subsequent paragraphs.

One needs to first identify the source of the susceptibility artifact, before finding a way to reduce it. Sometimes, metallic objects may be

located in the patient clothing and can be easily removed. In cases where the metallic object is located within the patient, e.g., postoperative spine with metal implants and joint replacement with metallic prosthesis, several other reduction

strategies can be adopted (Christina et al. 2011). The use of gradient-echo sequences causes severe susceptibility artifacts and should be avoided in these situations. Spin-echo sequences cause less severe artifacts and can be preferentially used in these cases, especially FSE sequences with short

echo times (Buckwalter et al. 2011) (Fig. 4.6). Other correction measures include using small field of view (FOV), increasing the receiver bandwidth, using high-resolution matrix and higher gradient strength (Lee et al. 2007). Aligning the frequency-encoding gradient along



Fig. 4.6 Susceptibility artifacts. (a) Lateral radiograph of the cervical spine shows implants from posterior spinal fixation. (b) Axial gradient-echo MR image shows severe

degradation of the image quality due to blooming. There is marked improvement in the image quality using (c) T1-W and (d) T2-W spin-echo sequences

the direction of the long axis of the pedicle screw can reduce susceptibility artifacts in patients with spinal instrumentation. The use of newer titanium alloy implants causes significantly less susceptibility artifacts (Rutherford et al. 2007). Metal susceptibility artifacts can also be reduced by the use of special dual-component implants

which are made of a paramagnetic material and have a diamagnetic coating.

Special changes in MRI techniques have also been extremely useful in dealing with metal susceptibility artifacts, especially in cases of joint imaging after metallic implants (Fig. 4.7). Although view-angle tilting (VAT) technique can significantly



Fig. 4.7 Susceptibility artifacts. (a) Sagittal fat-suppressed T2-W MR image of the lumbar spine shows prominent susceptibility artifacts due to metal implants.

These are reduced using (b) view-angle tilting (VAT). (c) There is however blurring and reduced SNR associated with VAT, as evident on increasing the bandwidth

reduce in-plane distortion artifacts, it does not correct the through-slice distortion. This technique adds a gradient of similar amplitude to the slice-select gradient on the slice-select axis during readout (Butts et al. 2005). The disadvantage of VAT is blurring of the image, which can be reduced by increasing the readout and reducing the excitation bandwidth. Slice encoding for metal artifact correction (SEMAC) and multi-acquisition variable-resonance image combination (MAVRIC) can be useful in imaging of patients with metallic joint implants (Koch et al. 2009; Lu et al. 2009; Lee et al. 2014). These techniques not only reduce the susceptibility artifacts but also improve the visualization of the metal-bone interface. This enables optimal evaluation, especially in cases with suspected infection. Images acquired using these techniques have been shown to be of similar quality as the conventional T1-weighted, T2-weighted, and proton density MR images (Singh et al. 2014). These techniques are superior to fast spin-echo sequences, in reduction of the susceptibility artifacts and also in measurements of the implant geometry.

MAVRIC limits the excitation bandwidth and uses several resonant frequency offset acquisi-

tions, in order to cover the entire spectral range. SEMAC builds on the VAT and corrects the image distortion and metallic susceptibility artifact. It uses a 3D spin-echo acquisition with an additional slice-encoding gradient, in addition to a conventional fast spin-echo sequence (Lee et al. 2013). SEMAC in combination with VAT can reduce both through-plane and in-plane distortion artifacts (Sutter et al. 2012). SEMAC and MAVRIC have also been used in a combination technique, known as MAVRIC-SL (Choi et al. 2015). These techniques have been useful for through-plane artifact reduction, where the metal is in a plane adjacent to the image plane. Iterative decomposition of water and fat with echo asymmetry and least-squares estimation (IDEAL) is another imaging technique that has been useful in MRI in cases with metallic devices (Reeder et al. 2005; Cha et al. 2011). This technique reduces the rim of hyperintense signal around the metallic device and also achieves uniform fat suppression (Cha et al. 2011) (Fig. 4.8). The associated image distortion however shows limited improvement. IDEAL is a Dixon-based technique to separate fat-only and water-only images. This technique



Fig. 4.8 Inhomogeneous fat suppression. (a) Sagittal fat-suppressed T2-W MR image of the lumbar spine shows inhomogeneous fat suppression, which is (b) reduced using the IDEAL technique

provides images with a high SNR and has been effectively used in T2-weighted and contrast-enhanced evaluation of the spine (Reeder et al. 2005; Shikhare et al. 2014). There is improved visualization of the spine and the adjacent structures, in addition to the reduction in metallic susceptibility artifacts and uniform fat suppression, around the metallic device.

4.2.3 Chemical Shift

Chemical shift phenomenon is also known as “misregistration” or “mismapping.” Different tissues have different chemical compositions and therefore have different resonating frequencies. The resonating frequency increases with increase in the strength of the external magnetic field (Peh and Chan 2001). Chemical shift artifacts are therefore stronger on 3 T imaging, as compared to MRI on a 1.5 T magnet (Dietrich et al. 2008). This artifact is characteristically seen in the frequency-encoding direction and arises as the

resonating frequency of fat is less than that of water. Chemical shift artifacts can be seen on all MR sequences and depend on the receiver bandwidth per pixel.

In MRI of the spine, chemical shift artifacts are seen as a hyperintense band on one side and as a hypointense band on the other side of a vertebral body (Fig. 4.9). The hyperintense band is typically seen at the overlapping interface of fat and water, while the hypointense band is seen at the region of the separating interface. These artifacts have been noted at several regions in spinal MRI. Chemical shift artifacts can be seen at the vertebral endplates, around the epidural fat and also around the ligamentum flavum (Fig. 4.10). These artifacts can also be seen around lipomatous and cystic lesions in the spine, such as lipoma or synovial cyst. Although chemical shift artifacts can result in loss of image quality due to superimposition of fat signal on surrounding structures, it has also been extremely useful in many ways.

Chemical shift artifacts have also been beneficial in abdominal imaging, for example, to characterize

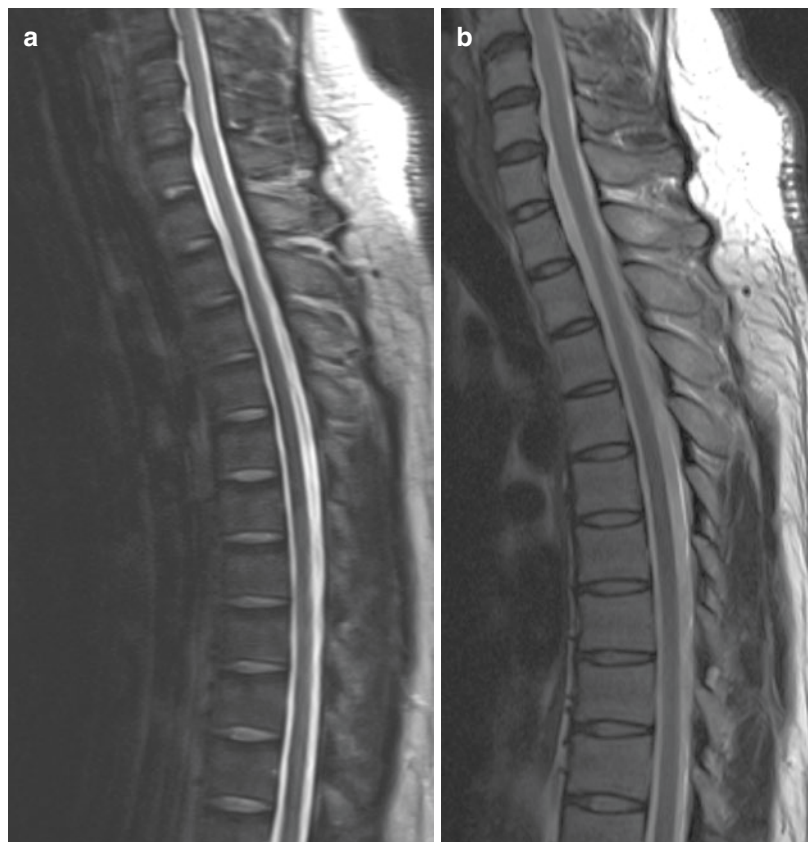


Fig. 4.9 Chemical shift artifact. (a) Sagittal T2-W MR image of the thoracic spine shows the chemical shift artifact as a dark band at the vertebral endplates, which (b) is reduced by increasing the bandwidth on the repeat MR image

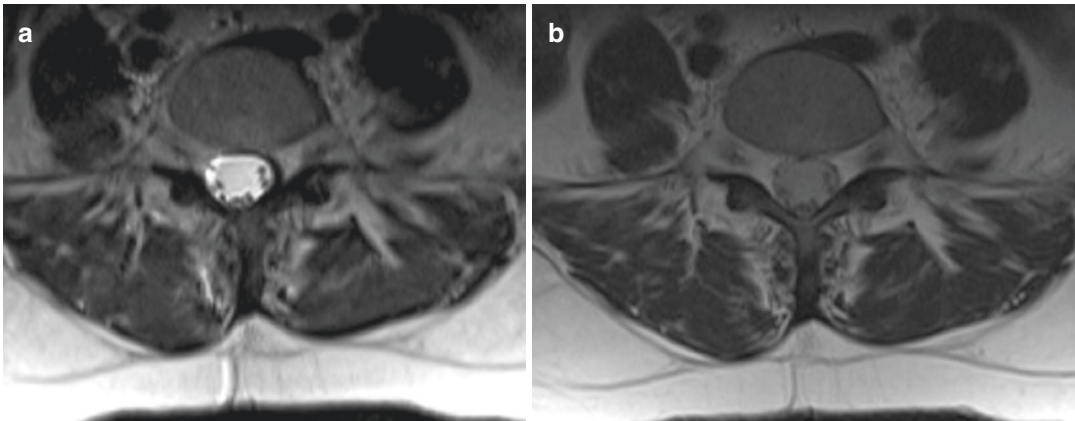


Fig. 4.10 Chemical shift artifact. (a) Axial T2-W MR image of the lumbar spine shows the chemical shift artifact which is seen as a dark band at the margins of CSF-fat

separation and as a bright band at the margins of CSF-fat overlap. (b) The artifact is reduced by increasing the bandwidth on the repeat MR image

the adrenal nodules, to look for hepatic steatosis, and to identify presence of fat in lesions. These artifacts may, however, cause problems while interpreting the MR images of the spine and may need to be reduced. Chemical shift artifacts depend on the bandwidth and can be reduced by increasing the receiver bandwidth per pixel (Peh and Chan 2001). These artifacts can also be reduced by decreasing the gradient strength and are hence less prominent on lower-field-strength machines. They can also be reduced by switching the phase- and frequency-encoding directions and by using fat-suppressed sequences (Singh et al. 2014).

4.2.4 Magic Angle Phenomenon

Dipolar interaction between two nuclei has angular dependence. This is especially important for tissues with a dense molecular structure such as collagen. The term “ $3\cos^2\theta-1$ ” modulates the dipolar interactions, where θ denotes angle of the structures with the static magnetic field (Bydder et al. 2007). The value of this equation becomes 0, when θ is approximately 54.7° (the magic angle). When the nuclei are oriented close to this magic angle, the dipolar interaction due to the static field is minimized, and the T2 value lengthens, resulting in a spurious signal on the MR image. Magic angle phenomenon is a unique artifact on MRI, seen on sequences using short echo time (TE), typically less than 36 ms. This artifact

can be seen on T1-weighted, gradient-echo, and proton density images. Magic angle artifacts occur in anisotropic structures, such as the tendons, ligaments, menisci, and hyaline cartilage (Singh et al. 2014). It can also be seen in intervertebral disks, fibrocartilage, and peripheral nerves. Magic angle phenomenon is not seen on sequences with a “critical” TE of more than 37 ms (Peh and Chan 1998).

The magic angle phenomenon involving the tendons, ligaments, or menisci produces an area of spurious hyperintense signal and hence may mimic pathology by simulating a tear, tendinopathy, or degeneration. Typical sites of this artifact include the supraspinatus tendon (Fig. 4.11), the triangular fibrocartilage complex of the wrist, the proximal posterior cruciate ligament, the infrapatellar tendon, and the Achilles tendon (Du et al. 2009) (Fig. 4.12). It can also be seen involving the peroneal tendons around the lateral malleolus (Mengiardi et al. 2006). This artifact can also cause simulation of a tear or degeneration of the articular cartilage of the knee (Disler et al. 2000; Xia 2000; Wang and Regatte 2015). Magic angle phenomenon can also cause pitfalls on MR neurography, a technique useful in the assessment of peripheral nerves and brachial plexus nerve roots (Chappell et al. 2004). Spurious hyperintense signal in the nerves can be misinterpreted as being due to an underlying disease (Kastel et al. 2011). A magic angle artifact can be reduced by using MR sequences with long TE, such as

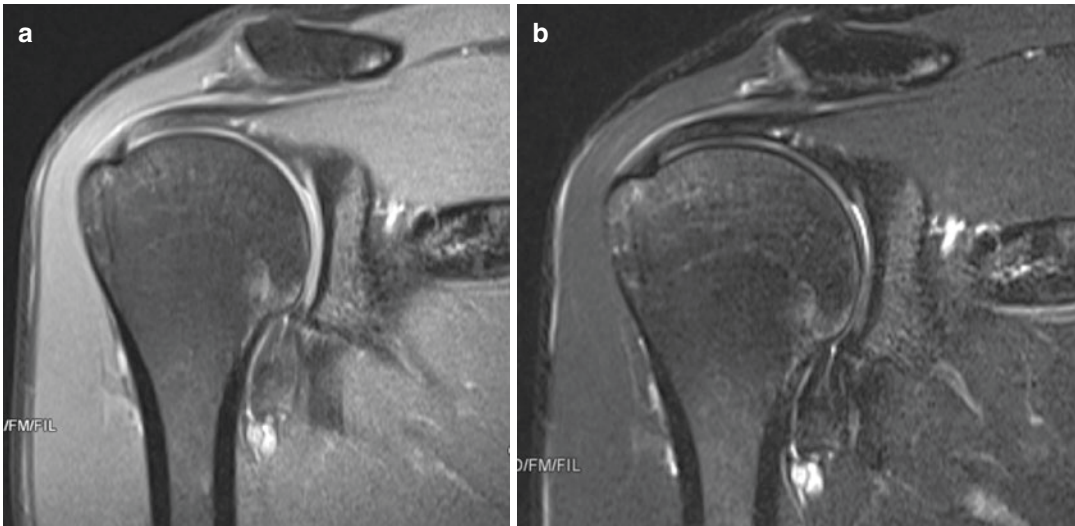


Fig. 4.11 Magic angle phenomenon. (a) Coronal fat-suppressed PD-W MR image of the shoulder shows an artifactual hyperintense signal in the supraspinatus tendon

due to the magic angle phenomenon. TE was 33 ms. (b) There is reduction of the artifact on the repeat coronal MR image obtained with a TE of 76 ms

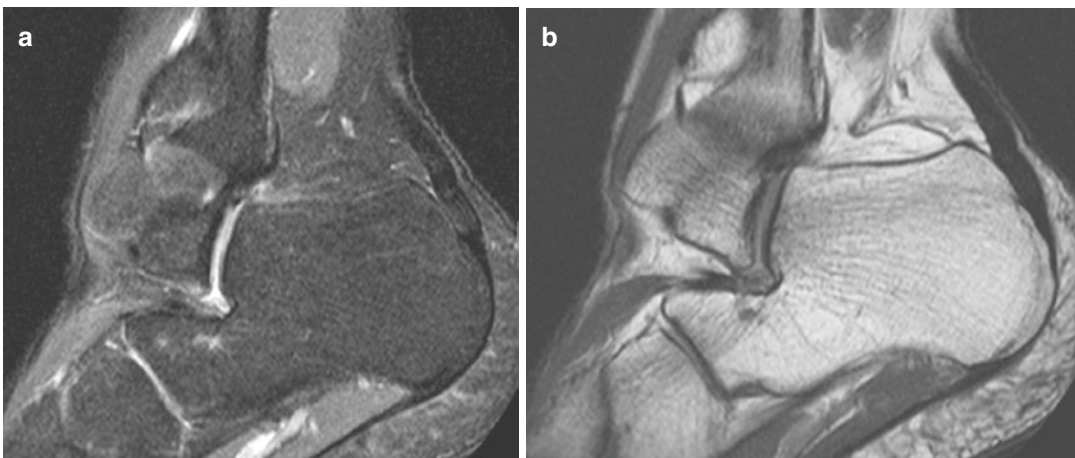


Fig. 4.12 Magic angle phenomenon. (a) Sagittal fat-suppressed PD-W MR image of the ankle shows spurious high signal in the Achilles tendon due to the magic angle

phenomenon. TE was 33 ms. (b) There is reduction of the artifact on the repeat sagittal MR image obtained after increasing the TE to >36 ms

T2-weighted images. The signal abnormalities seen on sequences with short TE can be compared with corresponding T2-weighted images. Persistent signal abnormality is indicative of pathology, while correction of the signal abnormality suggests magic angle phenomenon. These artifacts can also be corrected by repositioning the patient, as this changes the orientation of the structures to the main magnetic field (Peh and Chan 2001). External rotation of the arm has

been shown to reduce the magic angle artifact involving the supraspinatus tendon during MRI evaluation of the shoulder.

4.2.5 Protocol Errors

Protocol error artifacts include partial volume averaging, RF interference, saturation, shading, truncation, and wraparound and arise due to poor

planning or improper parameter selection during the MR scan. Avoiding these artifacts needs proper training and knowledge of the technicalities of MRI.

4.2.5.1 Partial Volume Averaging

This artifact is dependent on the voxel size or slice thickness used during MR scanning. When the selected slice thickness or voxel size is similar to or lesser than the imaged structure, the resulting signal comes entirely from the imaged structure. However, when the slice thickness or voxel size is larger than the imaged structure, the final signal is a combination of the signal from all the structures, within the voxel. This can result in problems in assessment of small structures. One good example would be assessment of pathology in small structures such as menisci or glenoid labrum. If a larger voxel size or slice thickness is

selected in imaging these structures, partial volume averaging artifact can easily mimic a radial meniscal tear or labral tear. It can also result in image distortion. These artifacts can be reduced by using thinner slices or by using a smaller FOV (Singh et al. 2014).

4.2.5.2 Radiofrequency Interference

RF interference is also known as “zipper artifact.” The artifact can arise due to external electromagnetic waves leaking within the scan room. These waves can arise from various sources, such as fluorescent lights, radio stations, electronic devices, static discharge, or even hardware dysfunction (Peh and Chan 2001). RF interference artifact results in spurious bands of varying signal intensity and are seen in a direction perpendicular to the frequency-encoding direction (Peh and Chan 2001) (Fig. 4.13).



Fig. 4.13 Radiofrequency interference artifacts. (a, b) Sagittal T2-W MR images of the thoracic spine show RF interference artifacts as spurious bands of varying signal intensity

4.2.5.3 Saturation

Saturation artifact arises due to intersection of the imaging slices with different obliquities (Peh and Chan 2001). This is typically due to poor planning and results in repeated RF excitation of the tissues, in the region of overlap. Simultaneous RF excitation of the overlapping slice occurs during the excitation of the first slice and causes reduction in the signal. This is seen as a hypointense band on the MR image, typically on axial imaging of the lumbar spine (Fig. 4.14). Saturation artifacts can

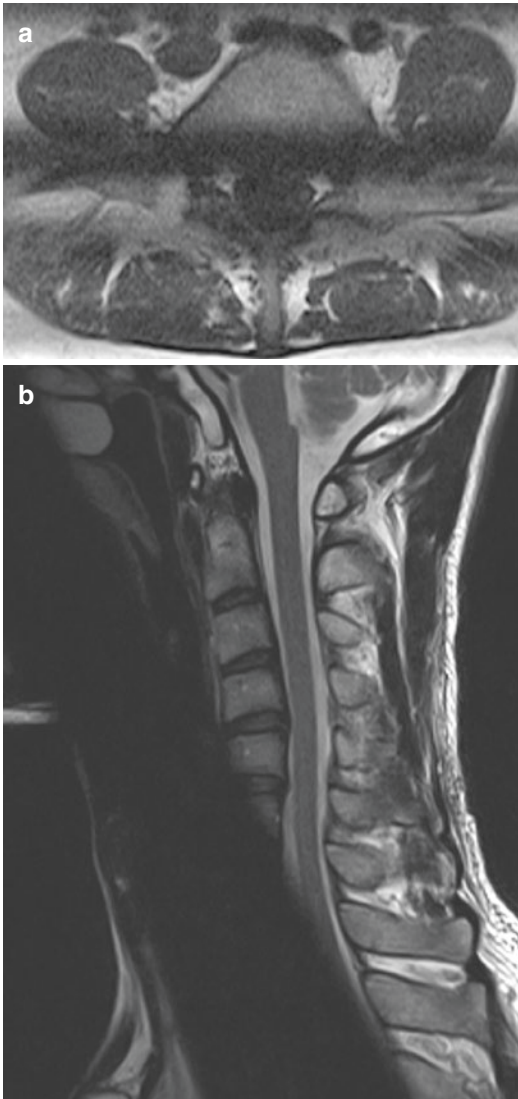


Fig. 4.14 Saturation artifact. (a) Axial T1-W MR image of the lumbar spine and (b) sagittal T2-W MR image of the cervical spine show the saturation artifact as a dark band partially obscuring the vertebral body

also been seen in MRI of the knee and can be seen in the region of the menisci. Proper planning during the MR scan is essential to correct this artifact. The simplest way is to avoid intersecting slices. If this is difficult to avoid, one has to try placing the zone of intersection away from the point of interest. Gradient-echo imaging can also be useful in reducing these artifacts as the tissue magnetization is only flipped by a small angle on gradient-echo sequences, thereby allowing easy recovery (Singh et al. 2014).

4.2.5.4 Shading

Shading artifact is seen as nonuniform signal intensity across the MR image (Fig. 4.15). This can be due to nonuniform excitation of the protons, resulting in inhomogeneous signal intensity across the image. Another cause of shading artifact is improper placement of the coils, resulting in uneven coverage of the region of interest (Smith and Nayak 2010). The resultant image shows areas of hypointense signal, characteristically located progressively further away from the coil. Shading artifact can also arise due to improper coupling of the coils, leading to signal loss at the coupling point. Inhomogeneity of the RF field can also result in loss of signal, thereby causing this artifact. Shading artifacts are problematic, as they can result in signal loss, variable image contrast, and loss of brightness. The artifact is worse in regions further away from the coil, commonly seen with the use of surface coils.



Fig. 4.15 Shading artifact. Axial T1-W MR image of the lumbar spine shows a gradual reduction in image brightness and contrast, toward the left side, due to the shading artifact

Reduction of shading artifact requires identification of its cause. In cases of improper coil placement or improper coupling, readjustment of the coils can eliminate this artifact. One needs to ensure that there is no direct contact between the patient and the coil. This can be achieved by placing water bags or foam pads separating the coil from the patient. In larger patients, the use of a larger surface coil or an enclosing coil can be useful. In cases where the artifact persists even on readjusting or checking the coil placement, changing the coil has to be considered. Surface coil intensity correction has also been found useful to limit these artifacts (Smith and Nayak 2010). Proper shimming techniques, such as active or passive shimming, can be useful to limit shading artifacts. These artifacts can also be limited by the use of RF pulses that are non-dependent on the field homogeneity.

4.2.5.5 Truncation

These artifacts are also called as “ringing” or “Gibbs phenomenon” and appear as parallel lines in region of a high-contrast interface. These artifacts can result in a false hyperintense signal involving the spinal cord, which can be misinterpreted as cord edema, syrinx, or myelomalacia (Fig. 4.16). To avoid the truncation artifacts, one needs to increase the matrix or decrease the FOV, if possible. Fat-suppression techniques can also be useful in reducing truncation artifacts.

4.2.5.6 Wraparound

Wraparound artifact is a protocol error artifact and is also known as aliasing artifact (Fig. 4.17). It is seen when the imaging FOV is smaller than the imaged body part (Peh and Chan 2001). The simplest way to correct this artifact is to increase



Fig. 4.16 Truncation artifact. (a) Sagittal T2-W MR image of the cervical spine shows linear hyperintense signal mimicking a syrinx in the spinal cord. (b) The trunca-

tion artifact is reduced by increasing the matrix size on the repeat sagittal MR image

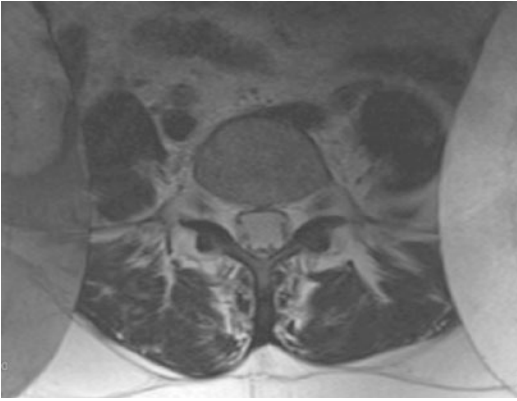


Fig. 4.17 Wraparound artifacts seen on axial T2-W MR image of the lumbar spine

the FOV. One can also switch the phase- and frequency-encoding gradients with the use of a rectangular matrix, if the geometry allows it. Saturation techniques can also be used to limit the wraparound artifacts arising from structures outside the desired FOV. These artifacts can also be overcome by the “no phase wrap” technique, without any increase in scan time or loss of spatial resolution. This may, however, result in reduced SNR. This “no phase wrap” technique doubles the FOV in the phase-encoding direction with doubling of the phase-encoding steps, thus maintaining the spatial resolution (Peh and Chan 2001).

4.3 Technical Pros and Cons

4.3.1 Fat-Suppression Techniques

The signal produced during MRI is mainly contributed by the hydrogen nuclei from water and fat. The signal from the fat molecules in adipose tissue needs to be suppressed in many situations, especially during musculoskeletal imaging. This needs good fat-suppression techniques, which also improve the image contrast. Water and fat have different resonant frequencies, and a fat-suppression module can be inserted at the beginning of an MR sequence in order to suppress the fat signal. A number of fat-suppression techniques are available, each with distinct pros and

cons. Spectral fat suppression, STIR (short T1 inversion recovery), and DIXON are the main fat-suppression techniques. Spectral fat saturation is a frequency-dependent technique, and fat is suppressed by a frequency-selective saturation pulse, followed by spoiling gradients, to dephase the fat signal (the latter is not mandatory). The water signal is however not affected. The separation of water and fat is twice at 3 T compared to 1.5 T, but susceptibility artifacts partially “eat up” this advantage. The technique is susceptible to main magnetic field inhomogeneity and has a limited role in postoperative imaging in the presence of metallic implants. One advantage of this technique is that the SNR is preserved.

STIR is a relaxation-dependent technique and uses a value of the TI (inversion time) so that the fat signal is nulled. The resultant fat void image is inherently T1 weighted with inversion of the T1 contrast. This technique has a longer acquisition time and is sensitive to B1 (RF) inhomogeneity. The SNR is reduced using this technique. The advantage of this technique is that it is insensitive to the main magnetic field inhomogeneity. It can therefore be effectively used in cases with metallic implants (Fig. 4.18). It is also useful in low-field-strength and poorly shimmed magnets. DIXON is a phase-dependent technique and works on the fact that fat and water precess at different rates in the transverse plane, as they have different Larmor frequencies (Fig. 4.19). Two separate images can be acquired by adjusting the sequence timing, with water and fat protons in phase and opposed phase. Averaging the sum and the difference yields “pure water” and “pure fat” images.

4.3.2 Isotropic Imaging

Musculoskeletal MRI has conventionally been performed using two-dimensional (2D) multislice acquisitions, especially FSE sequences. Although these sequences provide excellent images for diagnosing meniscal, ligamentous, and cartilage abnormalities, there are a number of drawbacks related to this technique. The main disadvantage is anisotropic voxels with relatively thick slices, as

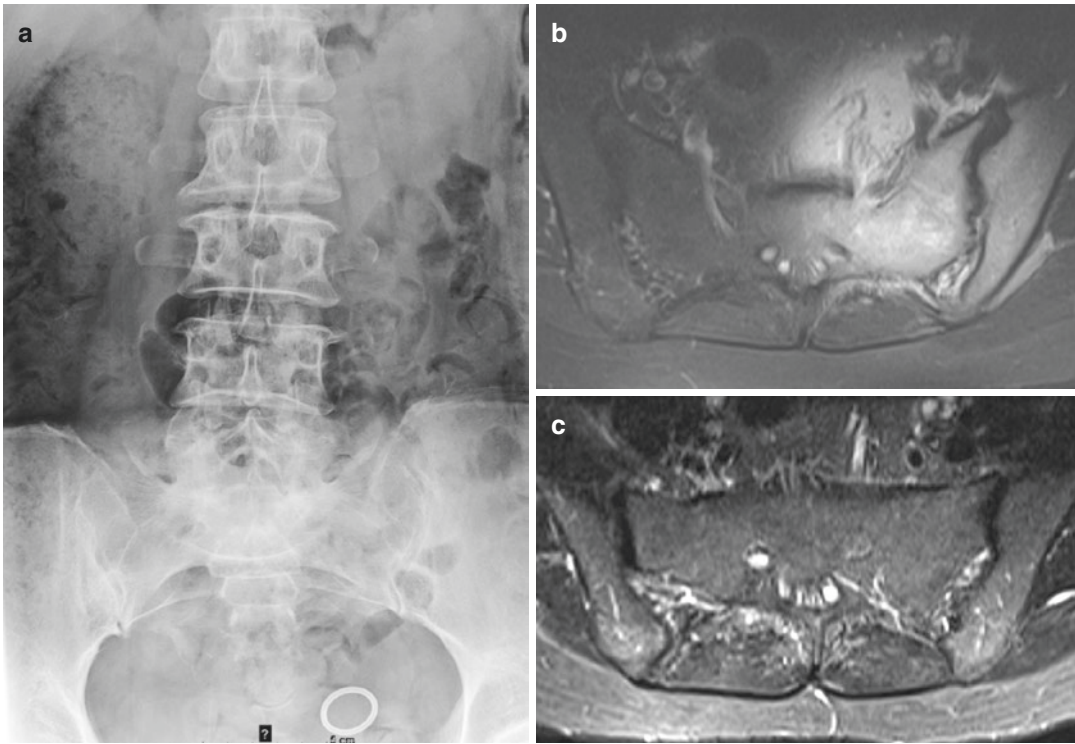


Fig. 4.18 Incomplete fat suppression due to a metallic object. (a) Frontal lumbar spine radiograph shows a contraceptive device projected over the pelvic cavity. (b) Axial fat-suppressed T2-W MR image of the pelvis shows

incomplete fat suppression, resulting in artifactual signal abnormality involving the sacrum. (c) The artifact is reduced on repeat STIR imaging

compared to the in-plane resolution (Shapiro et al. 2012). This results in partial volume artifact. The images cannot be reformatted into different planes, and hence, separate image sets have to be acquired if visualization is needed in oblique planes. Volume calculations are also suboptimal using this method. These disadvantages are overcome with newer three-dimensional (3D) imaging techniques. Not only do these newer techniques allow multiplanar reconstructions, but they also allow accurate quantification of various important structures. The partial volume artifacts are also reduced, as thinner slices can be acquired. The overall scan time can also be reduced by reconstructing different planes from a single acquisition. 3D isotropic imaging provides thin contiguous slices, useful in MRI evaluation of the shoulder, wrist, knee, and ankle. The 3D technique also provides excellent fat suppression; however, the individual sequences have longer scan time.

Several 3D sequences are routinely used in musculoskeletal imaging. T1-weighted spoiled gradient-recalled echo (SPGR), dual-echo steady-state (DESS), steady-state free precession (SSFP), and FLASH are some of the 3D gradient-echo sequences that are especially useful in assessment of the articular cartilage (Naraghi and White 2012). These are however limited in patients with metallic implants, as these sequences are more prone to susceptibility artifacts. There is also an increase in the scan time. Magic angle phenomenon is a problem on SSFP sequences. Sampling perfection with application-optimized contrast with different flip angle evolutions (SPACE) and FSE cube acquisition are examples of 3D FSE sequences. One has to carefully plan the scanning protocols to incorporate the high-resolution 3D sequences, in addition to the 2D sequences. This will limit the overall time penalty with the added advantages that the 3D sequences offer over conventional 2D ones.



Fig. 4.19 Incomplete fat suppression due to metallic implants. (a) Frontal and lateral radiographs of the ankle show plating of the distal fibula. (b) Sagittal contrast-enhanced fat-suppressed T1-W MR image shows susceptibility artifacts from the distal fibular implants which

have resulted in inhomogeneous fat suppression. (c) There is marked improvement in the image quality of the repeat sagittal MR image obtained using the DIXON technique of fat suppression

Conclusion

MRI is prone to a number of artifacts. Some arise due to poor scan planning, while others are related to the patient, the MRI machine, or a number of external factors. These artifacts not only affect the image quality but also can

mimic pathology. Some of the artifacts can easily be mistaken for abnormal cord signal or even a meniscal or ligamentous injury. MRI artifacts related to metallic implants, especially in the joints and in the spine, can pose a significant challenge to the reporting radiologist. The

radiologist needs to be aware of all these artifacts and the measures needed to correct them, in order to provide an accurate diagnosis. This chapter has described the various artifacts and discusses the individual correction measures. We have also discussed the technical pros and cons in choosing various fat-suppression techniques, in addition to the advantages and disadvantages of 2D versus 3D MR sequences, and related artifacts.

References

- Bernstein MA, Huston J, Ward HA (2006) Imaging artifacts at 3.0T. *J Magn Reson Imaging* 24:735–746
- Buckwalter KA, Lin C, Ford JM (2011) Managing post-operative artifacts on computed tomography and magnetic resonance imaging. *Semin Musculoskelet Radiol* 15:309–319
- Butts K, Pauly JM, Gold GE (2005) Reduction of blurring in view angle tilting MRI. *Magn Reson Med* 53:418–424
- Bydder M, Rahal A, Fullerton GD et al (2007) The magic angle effect: a source of artifact, determinant of image contrast, and technique for imaging. *J Magn Reson Imaging* 25:290–300
- Cha JG, Jin W, Lee MH et al (2011) Reducing metallic artifacts in postoperative spinal imaging: usefulness of IDEAL contrast-enhanced T1- and T2-weighted MR imaging- phantom and clinical studies. *Radiology* 259:885–893
- Chappell KE, Robson MD, Stonebridge-Foster A et al (2004) Magic angle effects in MR neurography. *Am J Neuroradiol* 25:431–440
- Chavhan GB, Babyn PS, Jankharia BG et al (2008) Steady-state MR imaging sequences: physics, classification, and clinical applications. *Radiographics* 28:1147–1160
- Choi SJ, Koch KM, Hargreaves BA et al (2015) Metal artifact reduction with MAVRIC SL at 3-T MRI in patients with hip arthroplasty. *AJR Am J Roentgenol* 204:140–147
- Christina A, Chen BA, Chen W et al (2011) New MR imaging methods for metallic implants in the knee: artifact correction and clinical impact. *J Magn Reson Imaging* 33:1121–1127
- Deshmane A, Gulani V, Griswold MA et al (2012) Parallel MR imaging. *J Magn Reson Imaging* 36:55–72
- Dietrich O, Reiser MF, Schoenberg SO (2008) Artifacts in 3-tesla MRI: physical background and reduction strategies. *Eur J Radiol* 65:29–35
- Dietrich TJ, Ulbrich EJ, Zanetti M et al (2011) PROPELLER technique to improve image quality of MRI of the shoulder. *AJR Am J Roentgenol* 197:93–100
- Dislser DG, Recht MP, McCauley TR (2000) MR imaging of the articular cartilage. *Skeletal Radiol* 29:367–377
- Du J, Pak BC, Znamirowski R et al (2009) Magic angle effect in magnetic resonance imaging of the Achilles tendon and enthesis. *Magn Reson Imaging* 27:557–564
- Eggers G, Rieker M, Kress B et al (2005) Artefacts in magnetic resonance imaging caused by dental material. *MAGMA* 18:103–111
- Hargreaves BA, Worters PW, Pauly KB et al (2011) Metal-induced artifacts in MRI. *AJR Am J Roentgenol* 197:547–555
- Jiachen Z, Rao PG (2006) MR artifacts, safety, and quality control. *Radiographics* 26:275–297
- Kastel T, Heiland S, Baumer P et al (2011) Magic angle effect: a relevant artifact in MR neurography at 3T? *Am J Neuroradiol* 32:821–827
- Koch KM, Lorbiecki JE, Hinks RS et al (2009) A multi-spectral three-dimensional acquisition technique for imaging near implants. *Magn Reson Med* 61:381–390
- Lee MJ, Kim S, Lee SA et al (2007) Overcoming artifacts from metallic orthopedic implants at high-field-strength MR imaging and multi-detector CT. *Radiographics* 27:791–803
- Lee YH, Lim D, Kim E et al (2013) Usefulness of slice encoding for metal artefact correction (SEMAC) for reducing metallic artifacts in 3-T MRI. *Magn Reson Imaging* 31:703–706
- Lee YH, Lim D, Kim E et al (2014) Feasibility of fat-saturated T2-weighted magnetic resonance imaging with slice encoding for metal artefact correction (SEMAC) at 3T. *Magn Reson Imaging* 32:1001–1005
- Lu W, Pauly KB, Gold GE et al (2009) SEMAC: slice encoding for metal artifact correction in MRI. *Magn Reson Med* 62:66–76
- Mansson S, Muller GM, Wellman F et al (2015) Phantom-based qualitative and quantitative evaluation of artifacts in MR images of metallic hip prostheses. *Phys Med* 31:173–178
- Mengiardi B, Pfirrmann CW, Schottle PB et al (2006) Magic angle effect in MR imaging of ankle tendons: influence of foot positioning on prevalence and site in asymptomatic patients and cadaveric tendons. *Eur Radiol* 16:2197–2206
- Morelli JN, Runge VM, Ai F et al (2011) An image-based approach to understanding the physics of MR artifacts. *Radiographics* 31:849–866
- Naraghi A, White LM (2012) Three-dimensional MRI of the musculoskeletal system. *AJR Am J Roentgenol* 199:283–293
- Peh WCG, Chan JHM (1998) The magic angle phenomenon in tendons: effect of varying the MR echo time. *Br J Radiol* 71:31–36
- Peh WCG, Chan JHM (2001) Artifacts in musculoskeletal magnetic resonance imaging: identification and correction. *Skeletal Radiol* 30:179–191
- Reeder SB, Pineda AR, Wen Z et al (2005) Iterative decomposition of water and fat with echo asymmetry and least-squares estimation (IDEAL): application with fast spin-echo imaging. *Magn Reson Med* 54:636–644
- Rumpel H, Chong Y, Porter DA et al (2013) Benign versus metastatic compression fractures: combined diffusion-

- weighted MRI and MR spectroscopy aids differentiation. *Eur Radiol* 23:541–550
- Rutherford EE, Tarplett LJ, Davies EM (2007) Lumbar spine fusion and stabilization: hardware, techniques, and imaging appearances. *Radiographics* 27:1737–1749
- Shapiro L, Harish M, Hargreaves B et al (2012) Advances in musculoskeletal MRI: technical considerations. *J Magn Reson Imaging* 36:775–787
- Shikhare SN, Singh DR, Peh WCG (2014) Variants and pitfalls in MR imaging of the spine. *Semin Musculoskelet Radiol* 18:23–35
- Singh DR, Chin MS, Peh WCG (2014) Artifacts in musculoskeletal MR imaging. *Semin Musculoskelet Radiol* 18:12–22
- Smith TB, Nayak KS (2010) MRI artifacts and correction strategies. *Imaging Med* 2:445–457
- Sutter R, Ulbrich EJ, Jellus V et al (2012) Reduction of metal artifacts in patients with total hip arthroplasty with slice-encoding metal artifact correction and view-angle tilting MR imaging. *Radiology* 265:204–214
- Tamhane AA, Arfanakis K (2009) Motion correction in periodically-rotated overlapping parallel lines with enhanced reconstruction (PROPELLER) and turbo-prop MRI. *Magn Reson Med* 62:174–182
- Tamhane AA, Arfanakis K, Anastasio M et al (2012) Rapid PROPELLER-MRI: a combination of iterative reconstruction and under-sampling. *J Magn Reson Imaging* 36:1241–1247
- Wang L, Regatte RR (2015) Investigation of regional influence of magic-angle effect on t2 in human articular cartilage with osteoarthritis at 3T. *Acad Radiol* 22:87–92
- Xia Y (2000) Magic-angle effect in magnetic resonance imaging of articular cartilage: a review. *Invest Radiol* 35:602–621